

Supplementary Material.

NMR relaxation studies of an RNA-binding segment of the Rous sarcoma virus Gag polyprotein in free and bound states - a model for autoinhibition of assembly

Gwen M. Taylor¹, Lixin Ma¹, Volker M. Vogt² and Carol Beth Post¹

¹Department of Medicinal Chemistry and Molecular Pharmacology, Markey Center for Structural Biology and Purdue Cancer Center, Purdue University, West Lafayette, Indiana

47907

²Department of Molecular Biology and Genetics, Cornell University, Ithaca, New York 14853

keywords: retrovirus, virus assembly, gag polyprotein, multidomain protein dynamics

Spectral density mapping for unbound and (GT)₄ bound CTD-SP-NC

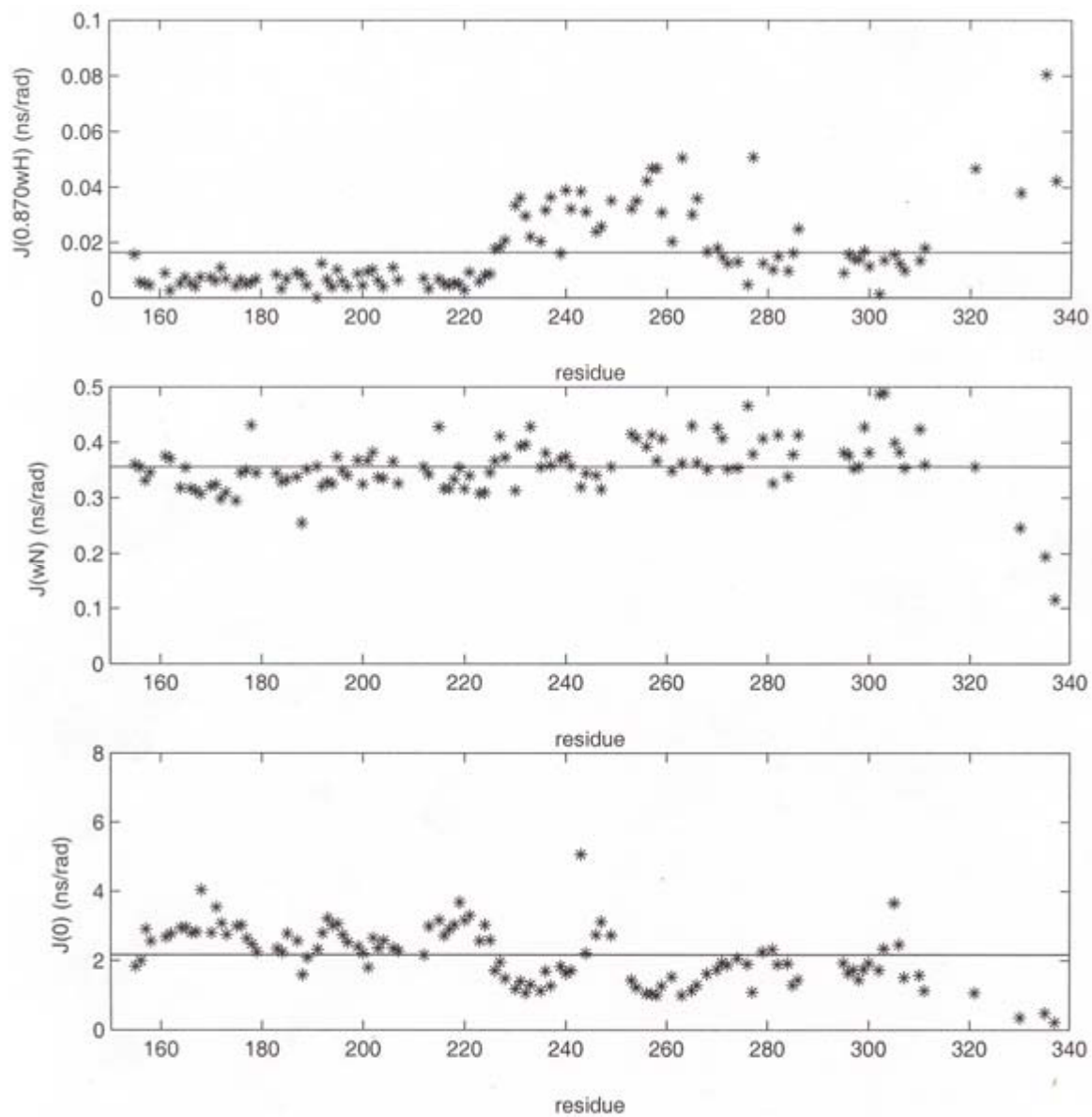
Main chain dynamics of CTD-SP-NC measured by ¹⁵N heteronuclear relaxation were characterized by spectral density mapping(*I*), a structure-independent approach, and the results are shown in Supplementary Figures 1 and 2. Averages over regions grouped based on relaxation behavior are listed in Supplementary Tables 1 and 2.

Dynamics of SP and flanking region in unbound CTD-SP-NC

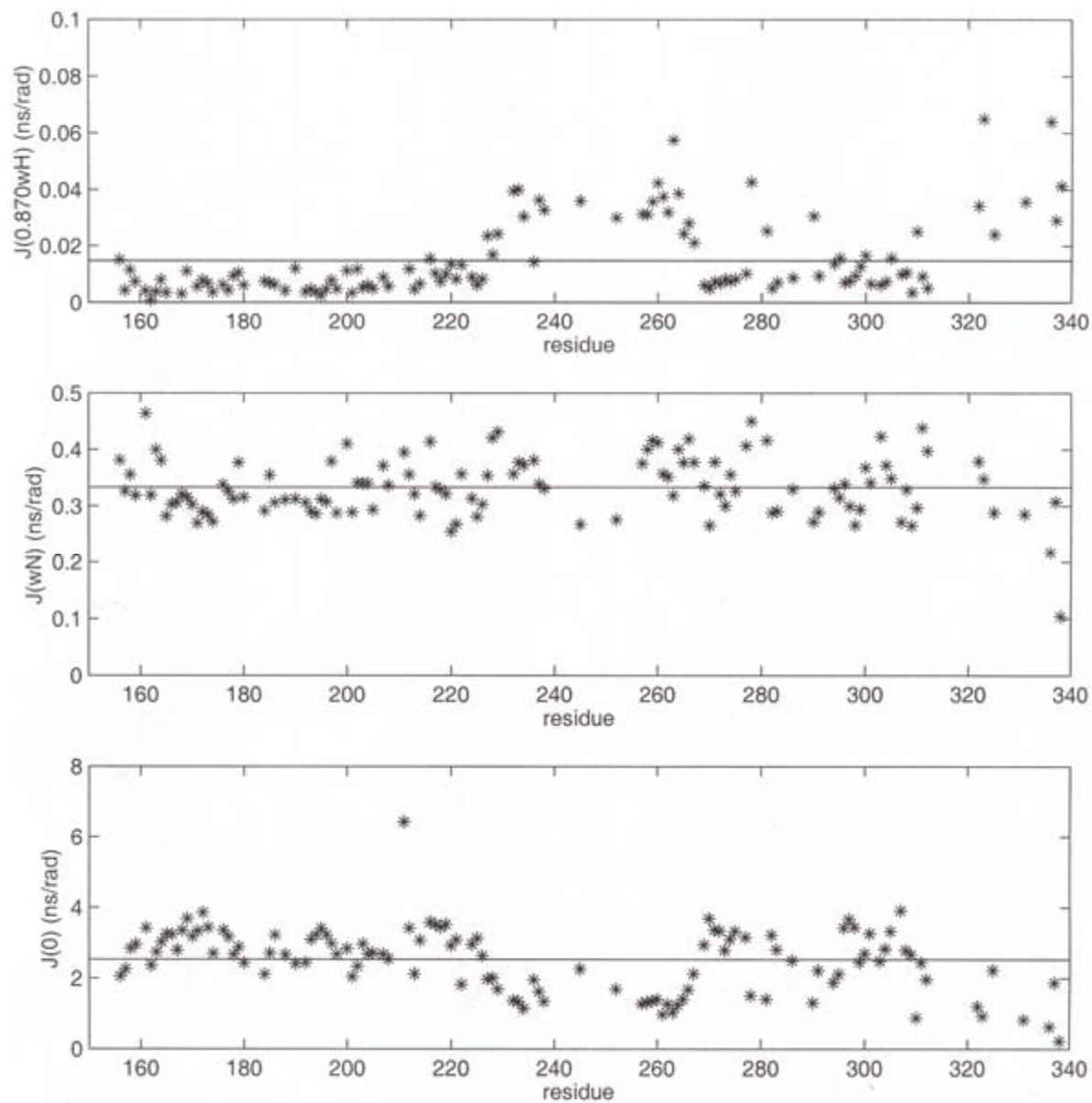
Theoretical curves for R_2 and R_1 as a function of overall correlation time are shown in Supplementary Figure 3 for the four motional models described in the article. Anisotropic rotation, shown in the left panel for axially symmetric rotation, affects the value of R_2 opposite in direction to that of R_1 . Internal motion decreases both relaxation rates.

A general description of the dynamics of SP and flanking regions is concluded based on the combined average values measured for I/I_0 , and R_1 and R_2 . The observed average value is $I/I_0 \sim 0$. Neither model 2 (anisotropic rotation) nor model 3 (very fast internal motion, single overall correlation time) can account for the observation that $I/I_0 \sim 0$. For model 1, $I/I_0 \sim 0$ occurs at $\tau_m = 1$ ns, a relatively short correlation time corresponding to a fully flexible linker. This value $\tau_m \sim 1$ ns falls to the left of the R_1 maximum so that the predicted R_1 and R_2 would be similar in value (for $\tau_m = 1$ ns, $R_1 = 2.0$ and $R_2 = 2.5$ s⁻¹). For model 4, R_2 is greater than R_1 and we use the example $S^2 = 0.5-0.6$, $\tau_{int} \sim 0.4$ ns, $\tau_m = 5 - 7$ ns for the predicted R_1 and R_2 values listed in Supplementary Table 4. For SP and flanking regions, the observed R_1 ranges from 1.8 – 2.1 s⁻¹ and R_2 ranges from 6 – 13 s⁻¹. While R_1 cannot readily discriminate models 1 and 4, the observed R_2 values are significantly greater and more variable than the values expected for model 1 and a fully flexible chain characterized by $\tau_m \sim 1$ ns. Model 4 more closely reproduces the overall relaxation behavior of the SP and flanking region; however, experimental R_2 values for several residues are underestimated by the theoretical relaxation curves. That R_2 values for this region are underestimated suggests that exchange (R_{ex}) contributes to R_2 .

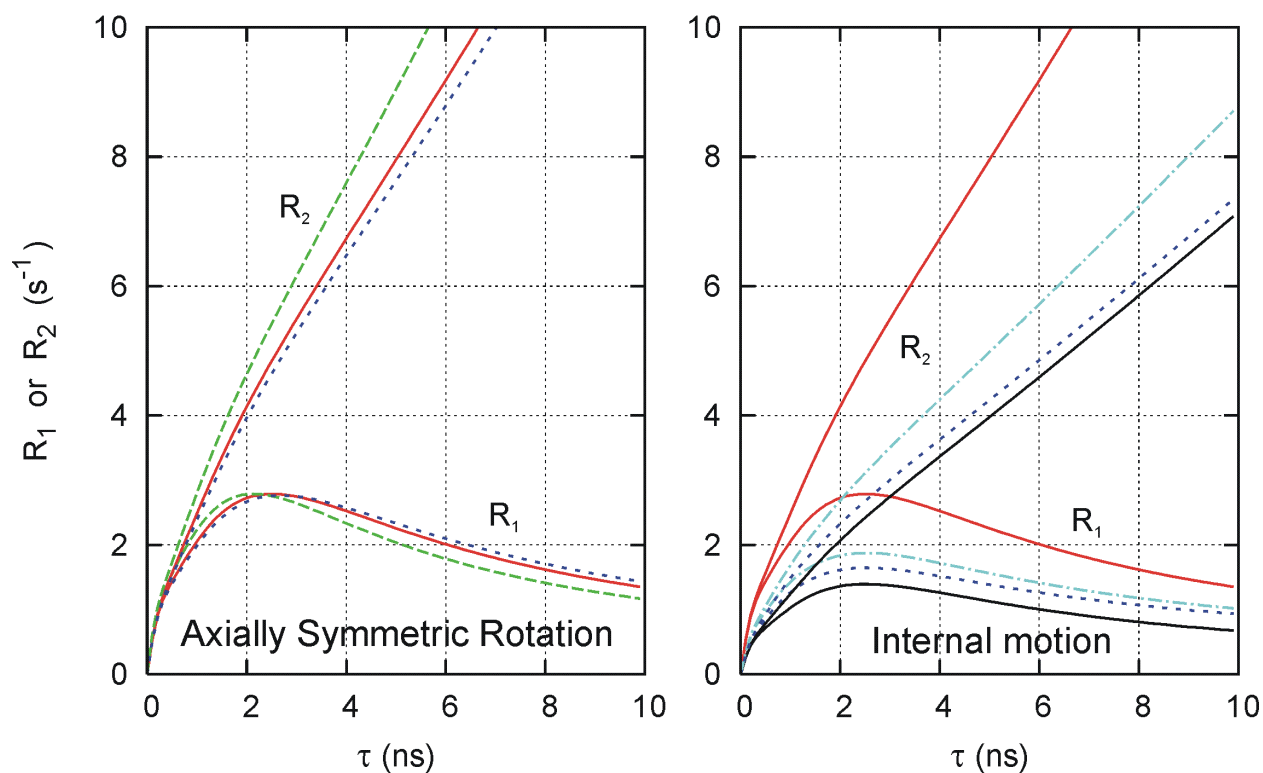
1. Peng, J. W., and Wagner, G. (1992) Mapping of the spectral densities of nitrogen-hydrogen bond motions in Eglin c using heteronuclear relaxation experiments, *Biochemistry* 31, 8571-8586.



Supplementary Figure 1. Spectral density mapping of RSV CTD-SP-NC in the apo form at 11.74 T. The average $J(0.87\omega H)$ is 1.64×10^{-11} , $J(\omega N)$ is 3.33×10^{-10} , and $J(0)$ is 2.16×10^{-9} .



Supplementary Figure 2. Spectral density mapping of RSV CTD-SP-NC in the bound form at 11.74 T. The average $J(0.87\omega_H)$ is 1.47×10^{-11} , $J(\omega_N)$ is 3.33×10^{-10} , and $J(0)$ is 2.52×10^{-9} .



Supplementary Figure 3. R_2 and R_1 as a function of overall correlation time, τ_m , for four motional models. Model 1, isotropic rotation with a single overall rotational correlation time (solid, red) is shown in both panels for reference. Left panel: Axially symmetric rotation with $D_{zz} = D_{\parallel} = 1.3$ and $D_{xx} = D_{yy} = D_{\perp} = 0.85$, and $\tau_m = 1/\left[2(D_{xx} + D_{yy} + D_{zz})\right]$. Two curves delimit the relaxation for N-H bond vectors aligned parallel (dashed, green) or perpendicular (dotted, blue) to the z-axial component of the diffusion tensor. Right panel: Overall isotropic rotation with faster internal motion. Model 3, a single correlation function including very fast internal motion squares, $S^2 = 0.5$ (solid, black). Model 4, internal motion with $\tau_{int} = 0.1$ ns and $S^2 = 0.6$ (dash-dot, cyan) or 0.5 (dotted, blue).

Supplementary Table 1. Average spectral density data for RSV CTD-SP-NC in the unbound state.

	residues	J(0) (ns/rad)	J(ω_N) (ns/rad 10 ⁻¹)	J(0.87 ω_H) (ns/rad 10 ⁻²)
CTD	394 - 474	2.5 ± 0.6	3.4 ± 0.3	0.9 ± 0.7
SP	475 - 489	2.4 ± 1.1	3.5 ± 0.2	3.1 ± 0.7
N-term NC	490 - 505	1.2 ± 0.2	3.9 ± 0.3	3.5 ± 1.1
NC core	509 - 548	1.9 ± 0.5	3.9 ± 0.4	1.5 ± 0.9
ZF 1	509 - 522	1.9 ± 0.4	3.9 ± 0.4	1.7 ± 0.1
ZF 2	535 - 548	2.0 ± 0.7	4.0 ± 0.5	1.2 ± 0.4

Supplementary Table 2. Average spectral density data for RSV CTD-SP-NC in the bound state.

	residues	J(0) (ns/rad)	J(ω_N) (ns/rad 10 ⁻¹)	J(0.87 ω_H) (ns/rad 10 ⁻²)
CTD	394 - 474	2.8 ± 0.8	3.3 ± 0.4	0.9 ± 0.8
SP	475 - 489	N.D.	N.D.	N.D.
N-term NC	490 - 505	1.7 ± 0.8	3.6 ± 0.5	3.0 ± 1.4
NC core	509 - 548	2.8 ± 0.7	3.3 ± 0.5	1.2 ± 0.9
ZF 1	509 - 522	2.8 ± 0.7	3.5 ± 0.6	1.3 ± 1.2
ZF 2	535 - 548	3.1 ± 0.5	3.2 ± 0.5	1.0 ± 0.4

Supplementary Table 3. S² values calculated by TENSOR

	residues	S ²
CTD	397 - 467	0.874
SP+flanking regions	468 - 507	
C-term CTD	468 - 477	
SP	479 - 493	
N-term NC	495 - 507	
NC core	509 - 548	0.642
ZF 1	509 - 522	0.707
ZF 2	535 - 548	0.671

Supplementary Table 4. Observed R_1 and R_2 values for SP* (residues 479 - 493) and the flanking regions (residues 468 - 477 and 495 - 507) compared to predicted values for model 1 or 4 at τ_m values with the condition III_0 is near zero.

	R_1 (s ⁻¹)	R_2 (s ⁻¹)
Observed		
Flanking C-term CTD	~2.2	~6.4
SP* ^c	1.8 to 2.2	6 to 13
Flanking N-term NC	~2.4	~5.5
Predicted		
Model 1, expected for $\tau_m = 1$ ns ^a	2.0	2.5
Model 4, expected for $\tau_m = 5-7$ ns ^b	1.9	4 to 7

^a Predicted values (Figure S3) calculated for a single overall correlation time, no internal motion.

^b Predicted values (Figure S3) calculated for slow internal motion parameters are $S^2=0.5$ to 0.6 and $\tau_{int}=0.4$ ns.

^c SP* residue range is based on relaxation behavior and differs somewhat from SP residues 477-488.